Monografías del Seminario Matemático García de Galdeano **31**, 509–518 (2004)

LOW MACH INVESTIGATION OF COMPRESSIBLE AIRFLOW AROUND A GENERIC AIRSHIP

Yacine Bentaleb, Eric Schall, Bruno Koobus and Mohamed Amara

Abstract. The numerical simulation of low Mach compressible flows around a generic airship is investigated using a Godunov-like numerical method. The hyperbolic differential problem -the three-dimensional Euler equations- is solved on unstructured meshes by a finite volume scheme based on Roe's upwind scheme [7] and Turkel's low Mach preconditioner [12, 5, 9, 10]. The effects of artificial viscosity and preconditioning on the computation of Drag and Lift coefficients are investigated. The classical Roe's scheme and its low Mach preconditioned variant are both considered using a sequence of three meshes of different fineness for solutions comparison and convergence. The numerical results show the preponderant part played by the low Mach preconditioner in terms of accuracy and robustness when very subsonic flows are considered, and the importance of using a small amount of numerical dissipation.

Keywords: Euler equations, Three-dimensional Compressible Flow, Low-Mach Number Preconditioning, Numerical dissipation, Finite Volume, Unstructured Grid.

AMS classification:

§1. Introduction

The prediction of aerodynamic forces is an important component in the study of airships. It allows, among others, to obtain some external informations for improving shape quality, adapting propulsion systems or to anticipate too large aeroelastic effects. In order to perform numerical simulations of flows around airships, a 6:1 prolate spheroid is chosen as reference configuration. One of the main difficulties in simulating compressible flows around airships is the low speed of the flow. When very subsonic compressible flows are solved by Godunov-like numerical methods, it becomes necessary to introduce a low Mach preconditioner. It consists in preconditioning the numerical dissipation in order to equilibrate the convective speed and the speed of sound, making them of the same order of magnitude, while the temporal and centered terms of the approximation remain unchanged. Then, the convergence to the steady state and the solution accuracy of the resulting preconditioned scheme are improved.

In the numerical simulations presented in this paper, the flow is considered non viscous and the hyperbolic differential problem defined by the Euler equations is solved on unstructured meshes by a finite volume method [3]. The differential equations are integrated over control volumes built from a finite element mesh, and across their interfaces an approximate Riemann solver based on Roe's scheme [7] with Turkel's low Mach preconditioner [12, 5, 9, 10] is used to evaluate the convective fluxes.

In this work, we are looking for the steady state solution around a prolate spheroid corresponding to an inflow Mach number of 0.1 and an angle of attack set to 5 degrees. Since the artificial viscosity is modified whereas the physical viscous effects are voluntarily neglected as a first approach, taking into account the contribution of the pressure force only, we propose to study the effects of the numerical dissipation on the evaluation of the aerodynamic coefficients with Roe's scheme and its low Mach preconditioned variant.

The remainder of this paper is organized as follows:

In Section 2, the governing equations are given. The numerical methodology is briefly described in Section 3. The test cases and the numerical results are presented in Section 4. Finally, we conclude this paper in Section 5.

§2. Governing equations

The three-dimensional Euler equations for fluid mechanics can be written in the following conservative form

$$\begin{aligned} \frac{\partial W}{\partial t} + \nabla \cdot \mathcal{F}(W) &= 0 \qquad t > 0 \text{ and } x \in \Omega \\ W(x,0) &= W_0(x) \qquad x \in \Omega \end{aligned} \tag{1}$$

where the conservative variable W and the inviscid flux vector $\mathcal{F} = (F, G, H)^T$ are given by

$$\begin{aligned} W &= (\rho, \rho u, \rho v, \rho w, E)^T \\ F(W) &= (\rho u, \rho u^2 + p, \rho uv + p, \rho uw + p, u(E+p))^T \\ G(W) &= (\rho v, \rho uv + p, \rho v^2 + p, \rho vw + p, v(E+p))^T \\ H(W) &= (\rho w, \rho uw + p, \rho vw + p, \rho w^2 + p, w(E+p))^T \end{aligned}$$

in which ρ denotes the density, u, v et w are the components of the velocity, and E is the total energy per unit volume. The following state equation for perfect gas connects the pressure p to the conservative variables and allows to close the system

$$p = (\gamma - 1)\left(E - \frac{1}{2}\rho(u^2 + v^2 + w^2)\right)$$

The ratio of the specific heats γ is fixed to 1.4.

For what concerns the boundary conditions, slip conditions are imposed on the body surface (here the prolate spheroid), and a representative far-field of the flow outside the computational domain is given.

§3. Numerical methodology

The spatial discretization of the Euler equations (1) is carried out here on an unstructured tetrahedral mesh from which a dual mesh defined by control volumes is derived (Fig. 1). The

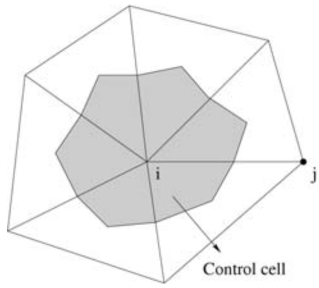

Figure 1: Control volume attached to vertex i in two dimensions.

convective fluxes are approximated by a finite volume method [3] in which the discretized solution is piecewise constant over each control volume. More specifically, Roe's upwind scheme with Turkel's low Mach preconditioner is used. The resulting scheme is refered as Roe-Turkel's scheme in the following. The convective fluxes are then approximated on the boundary of each control volume C_i attached to a vertex i as follows

$$\int_{\partial C_i} \mathcal{F}(W) \cdot n \, d\Gamma = \sum_{j \in V(i)} \Phi(W_i, W_j, \nu_{ij})$$

where n is the outer unit normal to the control volume C_i and $\nu_{ij} = \int_{\partial C_i \cap \partial C_j} n \, d\Gamma, \quad V(i)$ denotes the set of neighboring nodes to vertex i and $\Phi(W_i, W_j, \nu_{ij})$ are the numerical fluxes of Roe-Turkel's scheme given by

$$\Phi(W_i, W_j, \nu_{ij}) \; = \; \frac{\mathcal{F}(W_i) + \mathcal{F}(W_j)}{2} \cdot \nu_{ij} \; + \; \frac{1}{2} \, \delta \, P_c^{-1} \, | \, P_c \, D_c(\tilde{W}, \nu_{ij}) \, | \, (W_i - W_j) \tag{2}$$

in which $\tilde{W}$ denotes the Roe's average of W, $0 < \delta \leq 1$ is a real coefficient introduced to control the numerical viscosity, and D_c is the Roe's matrix given by

$$D_c(\tilde{W}, \nu_{ij}) = A_c(\tilde{W}) \, (\nu_{ij})_x + B_c(\tilde{W}) \, (\nu_{ij})_y + C_c(\tilde{W}) \, (\nu_{ij})_z \tag{3}$$

where A_c, B_c et C_c are the Jacobian matrices of the inviscid fluxes.
The preconditioning matrix P_c, proposed by Turkel [9], alter only the dissipative terms and thus the numerical scheme remains consistant with time-dependent equations. In terms of the entropic variables $U = [p, u, v, w, ln(p/(\rho^\gamma))]^T$, this preconditioner writes

$$P \; = \; Diag(\alpha^2, 1, 1, 1, 1)$$

where α is a parameter of the order of the reference Mach number.
Then, for the conservative variables W, the corresponding form of the preconditioner is
$P_c = \dfrac{\partial W}{\partial U} P \dfrac{\partial U}{\partial W}$

In order to improve the spatial approximation, second-order accuracy is obtained using the MUSCL technique [11, 3]. The numerical fluxes are evaluated with the extrapolated values W_{ij} and W_{ji} of W at the left and the right of the interface between two neighboring control volumes C_i and C_j. Thus, only the arguments of the numerical flux Φ are modified, while its expression (2) remains the same:

$$\int_{\partial C_i} \mathcal{F}(W) \cdot n \, d\Gamma \;=\; \sum_{j \in V(i)} \Phi(W_{ij}, W_{ji}, \nu_{ij}) \tag{4}$$

The extrapolated values W_{ij} and W_{ji} are computed using a "β-scheme", which combines centered and fully upwind gradients as follows

$$W_{ij} \;=\; W_i \;+\; \frac{1}{2}\left[(1-\beta)(\nabla W)^{cent}_{ij} + \beta(\nabla W)^{upw}_{ij}\right] \cdot \vec{ij} \tag{5}$$

$$W_{ji} \;=\; W_j \;-\; \frac{1}{2}\left[(1-\beta)(\nabla W)^{cent}_{ji} + \beta(\nabla W)^{upw}_{ji}\right] \cdot \vec{ij} \tag{6}$$

where $0 \leq \beta \leq 1$ is a parameter of upwinding.

The centered gradient associated with edge ij is defined by

$$(\nabla W)^{cent}_{ij} \cdot \vec{ij} = \; W_j - W_i \tag{7}$$

and the upwind gradients are given by

$$(\nabla W)^{upw}_{ij} \;=\; (\nabla W)\,|_{T_{ij}} \quad \text{and} \quad (\nabla W)^{upw}_{ji} \;=\; (\nabla W)\,|_{T_{ji}} \tag{8}$$

where T_{ij} and T_{ji} are respectively the upstream and downstream tetrahedra associated to edge ij (see Fig. 2 for the two-dimensional case) and $(\nabla W)\,|_T$ denotes the $P1$ finite-element approximation of the gradient in tetrahedron T.

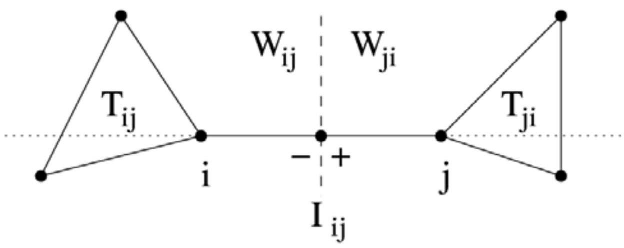

Figure 2: Upstream and downstream triangles T_{ij} and T_{ji} associated with edge ij.

Since the flow is subsonic, no slope-limiting procedure is used in the numerical fluxes.
For what concerns the time-integration strategy, a second-order time accurate implicit scheme is employed. The time discretization is based on a second-order backward difference scheme. The non-linear flow equations derived from the time-discretization are solved by a defect-correction (Newton-like) method [2].

§4. Numerical simulations

4.1. Test cases definition

The computations are performed on three meshes. The first one contains 33869 nodes and is considered as the coarse mesh (Fig. 9), the second one contains about three times more nodes while the third one contains four times more nodes and is considered as the fine mesh (Fig. 10). The surface mesh of the prolate spheroid is an unstructured triangulation following the prolate curvature, and the unstructured tetrahedral volume mesh connecting the bounding box to the surface mesh is generated by the Voronoi-Delaunay method [4].
In order to investigate the effects of the numerical viscosity on the evaluation of the Drag and the Lift coefficients, a truncation error analysis of the linear advection equation discretized on a regular structured grid allows to estimate the order of dispersion and dissipation. This analysis gives the first two preponderant terms (corresponding to a one-dimensional analysis for sake of briefness)

$$(1-3\beta)\ C_1\ \Delta_x^2\ \frac{\partial^3}{\partial x^3} \tag{9}$$

$$\delta\beta\ C_2\ \Delta_x^3\ \frac{\partial^4}{\partial x^4} \tag{10}$$

where the parameters β and δ have been previously defined.
The third order derivative term (9) represents the dispersive error while the dissipative term (10) is of fourth order.
The coefficient β controls the dispersion which is minimal for $\beta = 1/3$, value which is used for most of the test cases. The artificial viscosity can then be modified through the dissipative term and parameter δ. For our numerical study, we define a sequence of simulations by decreasing the value of the product $\delta\beta$ as follows

$$\left.\begin{array}{l}\beta = 1/2\\ \delta = 1\end{array}\right\} \Longrightarrow \delta\beta = 0.5 \qquad \left.\begin{array}{l}\beta = 1/3\\ \delta = 3/4\end{array}\right\} \Longrightarrow \delta\beta = 0.25 \qquad \left.\begin{array}{l}\beta = 1/3\\ \delta = 3/8\end{array}\right\} \Longrightarrow \delta\beta = 0.125$$

$$\left.\begin{array}{l}\beta = 1/3\\ \delta = 3/16\end{array}\right\} \Longrightarrow \delta\beta = 0.0625 \qquad \left.\begin{array}{l}\beta = 1/3\\ \delta = 3/32\end{array}\right\} \Longrightarrow \delta\beta = 0.03125$$

The inflow Mach number M_∞ is essentially fixed to 0.1. Computations corresponding to $M_\infty = 0.01$ are also performed in order to show the effect of preconditioning. Classical Roe's scheme and preconditioned Roe-Turkel's scheme are both performed and compared. The angle of attack is set to 5 degrees for each computation and the other reference quantities are

$$\begin{array}{rcl} l &=& 1.37\ m\\ \rho_\infty &=& 1.225\ kg/m^3\\ p_\infty &=& 101300\ Pa \end{array}$$

where l is the main length of the prolate spheroid.

The Drag (Cx) and Lift (Cz) coefficients are defined for these computations by

$$C_i = \frac{1}{S_{ref}} \int_\Gamma C_p \overrightarrow{n} \cdot \overrightarrow{i} \, ds \qquad \overrightarrow{i} = \overrightarrow{x}, \overrightarrow{y}, \overrightarrow{z} \tag{11}$$

in which S_{ref} is a reference area (see Table 1), $\overrightarrow{n}$ denotes the unit normal of the surface element, and C_p is the pressure coefficient $C_p = \frac{p-p_\infty}{\frac{1}{2}\rho_\infty V_\infty^2}$

4.2. Numerical results

The behavior of the Drag (Cx) and Lift (Cz) coefficients with respect to different values of $\delta\beta$ parameter is shown in Figs. 3 and 4 for Roe-Turkel's scheme. As this parameter is reduced, Cx and Cz decrease almost linearly for the three meshes. For weak values of $\delta\beta$, the Lift and Drag coefficients converge towards a rather closed value with the medium and fine grids. Simulations were performed on the same sequence of meshes by Mezine and Abgrall using a preconditioned LDA (Low Diffusion Advection) system scheme for solving the Euler equations [1]. For comparison purposes, their results are also plotted in Fig. 3 (black points and squares). With the coarse mesh, they obtain $Cx = 3.96\ 10^{-3}$, a value which corresponds to a simulation with Roe-Turkel's scheme and $\delta\beta = 0.17$. With the two other finer grids, the Cx coefficients obtained by Mezine and Abgrall correspond to values which would have been obtained by Roe-Turkel's scheme and $\delta\beta = 0.15$.
As the behavior of the aerodynamic coefficients is linear, the retained coefficients for these simulations are extrapolated at zero numerical viscosity which corresponds to $\delta\beta = 0$. Table 1 displays these extrapolated coefficients obtained with the fine mesh for both Roe's and Roe-Turkel's schemes. We can compare these values with those of Mezine and Abgrall for the same mesh and the same reference areas.
In Fig. 5, we compare the results obtained by Roe's and Roe-Turkel's schemes on the chosen sequence of meshes. The difference between the Drag coefficients corresponding to these two schemes reduces with decreasing values of $\delta\beta$ parameter, and almost vanishes for the smallest value of $\delta\beta$ with the medium and fine meshes. This feature is no more true when the flow becomes very subsonic. Fig. 6 shows that even with small values of $\delta\beta$, this difference remains rather large at $M_\infty = 0.01$. This is confirmed by the Mach number isovalues on the finest grid in regions close to the edges for $M_\infty = 0.01$ (Fig. 7). As expected, one can also notice in Fig. 6 that the drag variation curve for Roe-Turkel's scheme is similar at $M_\infty = 0.1$ and $M_\infty = 0.01$, contrary to what we observe for Roe's scheme. These results are explained by the wrong asymptotic behavior of Roe's scheme with small Mach number inducing in particular an excessive viscosity on the momentum equations, drawback which is corrected by Turkel's preconditioner [12]. Pressure isovalues for $M_\infty = 0.1$ are depicted in Fig. 8. We notice, with Roe's scheme, oscillations which do not exist when Roe-Turkel's scheme is used. This feature is explained by the too weak viscosity introduced on the energy equation by Roe's scheme for low Mach number, which induces a lack of stability of this scheme for low speed flows, shortcoming which is corrected with Turkel's preconditioner [12].

§5. Conclusion

In this paper, the numerical simulation of low Mach compressible flows around a generic airship has been investigated using a finite volume method based on Roe's upwind scheme. The flow

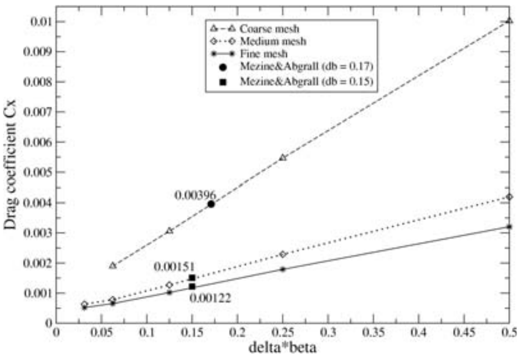

Figure 3: Drag coefficient versus $\delta\beta$ parameter using the Roe-Turkel's scheme.

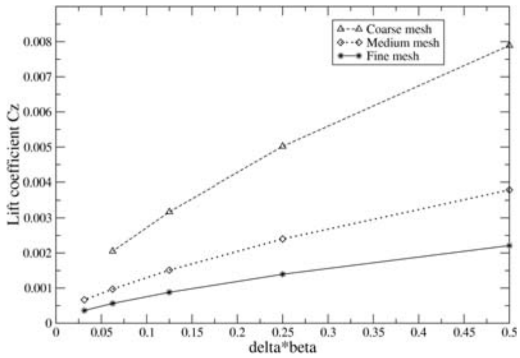

Figure 4: Lift coefficient versus $\delta\beta$ parameter using the Roe-Turkel's scheme.

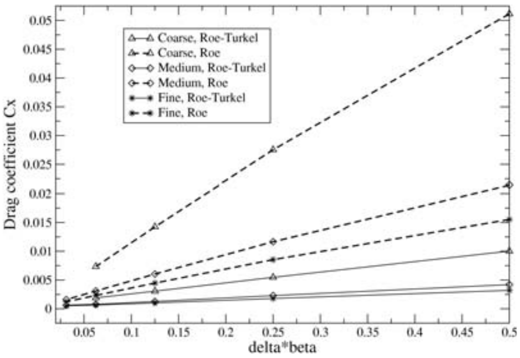

Figure 5: Drag coefficient versus $\delta\beta$; comparison between Roe's and Roe-Turkel's solver.

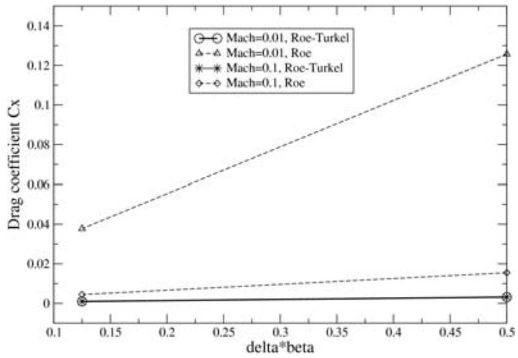

Figure 6: Influence of preconditioning on the Drag coefficient calculation for $M_\infty = 0.01$.

Solver	Drag coefficient	Lift coefficient
Roe	$1.2\ 10^{-4}$	$1.76\ 10^{-3}$
Roe-Turkel	$3.9\ 10^{-4}$	$1.6\ 10^{-4}$
Mezine & Abgrall	$1.22\ 10^{-3}$	$5.26\ 10^{-3}$
Reference areas	$\pi(1.37/12)^2$	$\pi(1.37)^2/24$

Table 1: Extrapolated Drag and Lift coefficients at zero numerical dissipation ($\delta\beta$ = 0) on the fine mesh (140265 nodes). The corresponding reference areas used in expression (11) are also given.

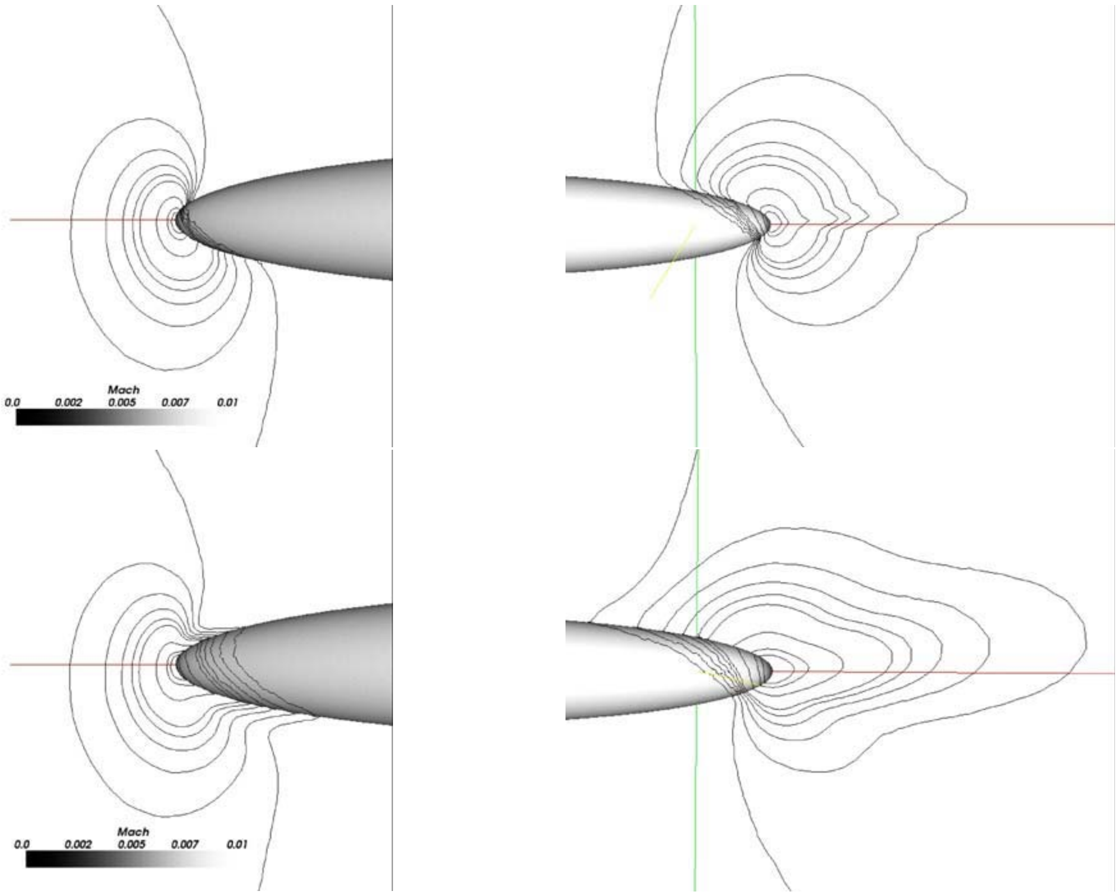

Figure 7: Isovalues of the Mach number for $M_\infty = 0.01$ and $\delta\beta = 0.125$ with Roe-Turkel's scheme (top) and Roe's one (bottom) on the fine mesh (140265 nodes).

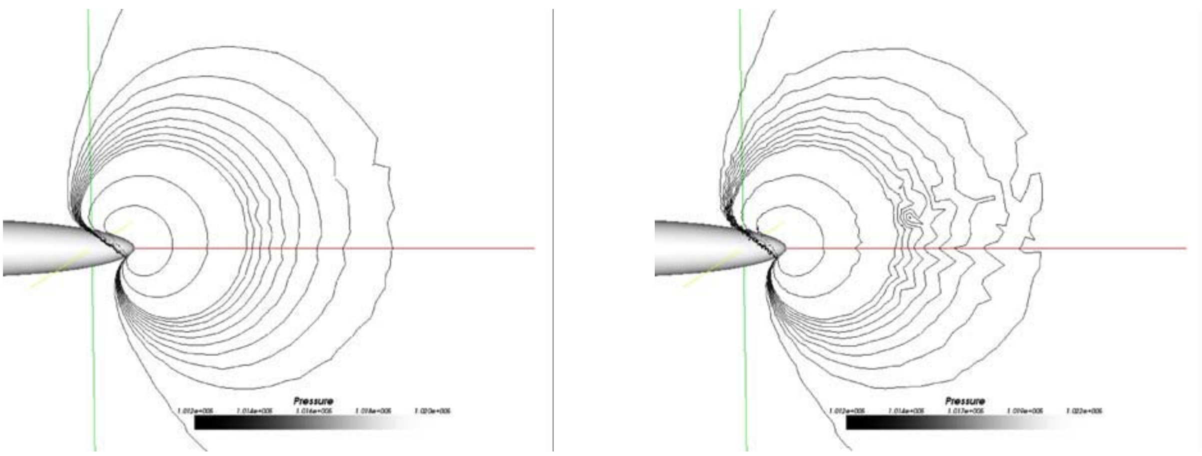

Figure 8: Isovalues of the pressure for $M_\infty = 0.1$ and $\delta\beta = 0.125$ with Roe-Turkel's scheme (left) and Roe's one (right) on the fine mesh (140265 nodes).

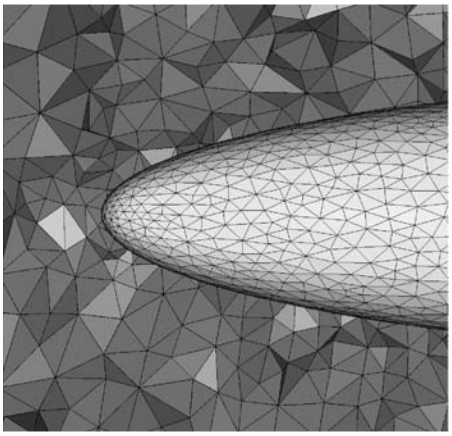

Figure 9: Coarse volume mesh: 33869 nodes.

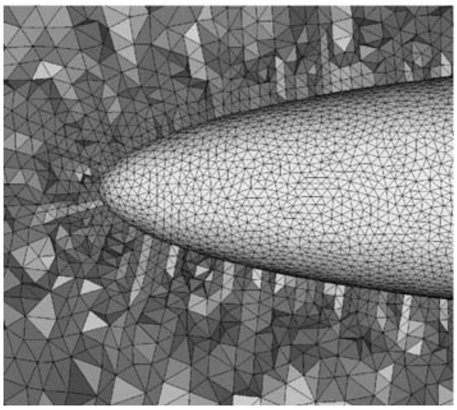

Figure 10: Fine volume mesh: 140265 nodes.

has been assumed non viscous and the Euler equations have been considered for this work. In order to address the difficulty of simulating low speed flows, Turkel's preconditioner has been used to modify the numerical viscosity which is, in our numerics, directly controled by a real parameter. We have studied the effects of both the preconditioner and the numerical dissipation through this real parameter on the evaluation of the aerodynamic coefficients. For this purpose, a sequence of three unstructured meshes of different fineness have been used. The numerical results have shown the crucial part played by the low Mach preconditioner for the simulation of very subsonic flows, and also the importance of using a small amount of numerical dissipation. Preconditioning enforces the robustness and improves the accuracy of the numerical scheme at low Mach number.
In the futur, we plan to perform the simulation of low speed turbulent viscous flows around a generic airship with the numerical methodology used in this paper for the discretization of the convective fluxes.

Acknowledgements

This work was supported by the Conseil Régional d'Aquitaine. The authors thank the Centre Informatique National de l'Enseignement Supérieur (CINES) for providing the computational resources.

References

[1] ABGRALL, R., AND MEZINE, M. Construction of second order accurate monotone and stable residual schemes: the steady case. *Journal of Computational Physics.* (2003).

[2] BOHMER, K.,HEMKER, P., AND STETTER, H. The Defect Correction Approach. *Comput. Supp.* (1984), 5:1–32.

[3] DERVIEUX, A. Steady Euler Simulations Using Unstructured Meshes. *Von Karman Institute Lecture Series.* (1985).

[4] GEORGE, P.L. Automatic mesh generation. Applications to finite element methods. *Wiley*, (1991).

[5] GUILLARD, H., AND VIOZAT, C. On the behavior of upwind schemes in the low Mach number limit. *Computers and Fluids. 28* (1997), 63–86.

[6] LARDAT, R., KOOBUS, B., RUFFINO, F., FARHAT, C., AND DERVIEUX A. Premières investigations du couplage fluide-structure autour d'un lanceur spatial générique. *Technical Report INRIA N°4314*, (2001).

[7] ROE, P.L. Approximate Riemann solver, parameters vectors and difference schemes. *Journal of Computational Physics. 43* (1981), 357–371 .

[8] SCHALL, E., VIOZAT, C., KOOBUS, B., AND DERVIEUX, A. Computation of Low Mach Flows with Implicit Upwind Methods. *International Journal of Heat and Mass Transfer.* (2003), accepted for publication.

[9] TURKEL, E. Preconditioned methods for solving the incompressible and low speed compressible equations. *Journal of Computational Physics. 72* (1987), 277–298.

[10] TURKEL, E. Review of preconditioned methods for fluid dynamics. *Applied Numerical Mathematics. 12* (1993), 257–284.

[11] VAN LEER, B. Towards the Ultimate Conservative Difference Scheme V: A Second Order Sequel to Godunov's Method. *Journal of Computational Physics. 32* (1979), 101–136.

[12] VIOZAT, C. Implicit Upwind Schemes for Low Mach Number Compressible Flows. *Technical Report INRIA N°3084*, (1997).

Yacine Bentaleb and Éric Schall
Laboratoire de Thermique, Énergétique et Procédés, EA 1932
Université de Pau et des Pays de l'Adour
IUT-GTE, 1 avenue de l'Université
64000 Pau, France
yacine.bentaleb@etud.univ-pau.fr and eric.schall@univ-pau.fr

Bruno Koobus
Laboratoire d'Analyse, Calcul Scientifique et Optimisation de Montpellier, FRE 2311 du CNRS
Université de Montpellier II
Département de Mathématiques, Case Courrier 51
34095 Montpellier Cedex 5, France
koobus@darboux.math.univ-montp2.fr

Mohamed Amara
Laboratoire de Mathématiques Appliquées, FRE 2570
Université de Pau et des Pays de l'Adour
I.P.R.A, B.P. 1155, 64013 Pau Cedex, France
mohamed.amara@univ-pau.fr